Photocatalysis

DOI: 10.1002/anie.200904876

Probing Photocatalytic Active Sites on a Single Titanosilicate Zeolite with a Redox-Responsive Fluorescent Dye**

Takashi Tachikawa, Soichiro Yamashita, and Tetsuro Majima**

Microporous titanosilicate ETS-10 is a promising material for applications such as adsorption, ion exchange, and (photo)catalysis because of 1) the inherent quantum nature of one-dimensional titania (-Ti-O-Ti-) wires in the framework and 2) its high reaction selectivity owing to its pore structure (dimensions of 0.8 nm × 0.5 nm).[1–3] In a defect-free crystal, charge carriers, that is, electrons and holes, are generated by the irradiation with photons with an energy corresponding to the band gap of approximately 4 eV. These carriers migrate in the crystal through the wires. However, the wires are broken at random points in the crystal because of inherent defects; these defects form active centers for molecular adsorption and redox reactions.[3–6] To date, the influences of structural defects in ETS-10 on the adsorption and reaction dynamics of organic compounds have not been well characterized, possibly because of the heterogeneous distribution of active sites in the material.

Herein, we describe the in situ fluorescence imaging of photocatalytic oxidation on single ETS-10 crystals using a redox-responsive fluorescent dye, 3′-(*p*-aminophenyl)fluorescein (APF, Figure 1 A). APF, which was originally developed as a fluorescent probe for selective detection of the hydroxyl radical (•OH) or hypohalites,[7] was employed to identify the surface active sites distributed over the ETS-10. It was revealed that surface treatment of ETS-10 with diluted aqueous hydrofluoric acid (HF) significantly increased not only the adsorption and reaction efficiencies but also the heterogeneity of photocatalytic activity among the crystals. Furthermore, we confirmed that crystal defects serve as active sites during the photocatalytic reaction in aqueous solution.

We first tested the photocatalytic activity of samples at the bulk level. Synthetic procedures and structural characterization of ETS-10 materials are provided in the Supporting Information. As shown in Figure S3 A in the Supporting Information, the fluorescence intensity of fluorescein increased gradually upon UV irradiation of phosphate buffer solutions (pH 7.4) containing APF (500 nM) and ETS-10 powder (0.5 mg mL^{-1}). In the absence of ETS-10, the fluorescence intensity did not increase at all, thus suggesting that fluorescein molecules might be generated by the reaction of photoexcited ETS-10 and APF molecules. Meanwhile, as expected, a significant increase in the fluorescence intensity was observed for HF-treated ETS-10 because of the exposure of surface active sites such as titanols and larger micropores (supermicropores) by partial dissolution of siliceous walls surrounding the titania wires.[3] It was estimated that approximately 70 % of fluorescein molecules were generated by a bimolecular reaction with •OH using DMSO as a scavenger (Figure S3 in the Supporting Information).

Before performing the imaging study for single ETS-10 crystals, we examined the redox responsiveness of APF using an in situ spectroelectrochemical technique combined with total internal reflection fluorescence microscopy (TIRFM, Figure 1 B).[8] According to the literature,[7a] the fluorescence of APF in aqueous solution is almost completely quenched by

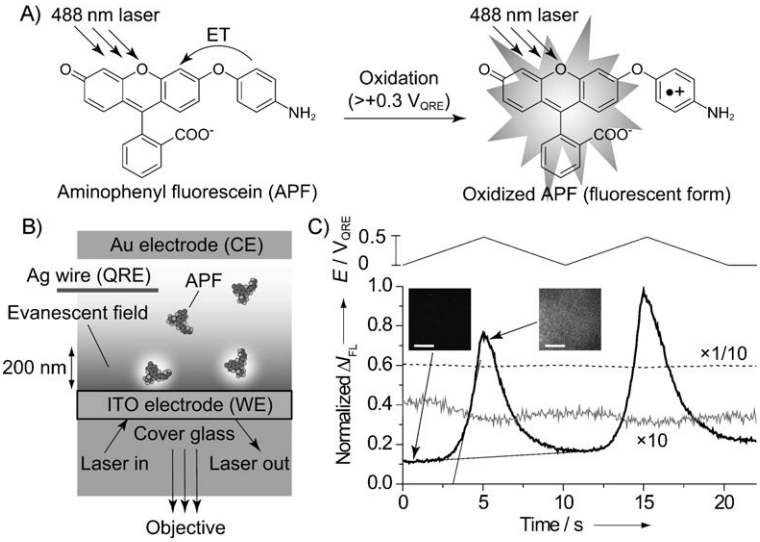

Figure 1. A) Reaction scheme for the one-electron oxidation of the *p*-aminophenyl moiety, which induces fluorescence in APF. ET = electron transfer. B) Cell configuration for in situ spectroelectrochemical measurements under TIRFM. CE = counter electrode, QRE = quasi-reference electrode, WE = working electrode. C) Applied potential dependence of normalized fluorescence intensity (I_{FL}) obtained for the phosphate buffer solutions in the absence (gray line) and presence of APF (5 μM; solid line) or fluorescein (500 nM; dashed line). The images in (C) were acquired at a bin time of 50 ms. Scale bars are 5 μm.

[*] Dr. T. Tachikawa, S. Yamashita, Prof. Dr. T. Majima
The Institute of Scientific and Industrial Research (SANKEN)
Osaka University, Mihogaoka 8-1, Ibaraki, Osaka 567-0047 (Japan)
Fax: (+81) 6-6879-8499
E-mail: tachi45@sanken.osaka-u.ac.jp
majima@sanken.osaka-u.ac.jp

[**] We are grateful to Mr. Kazuya Naito for his experimental assistance. This work has been partly supported by a Grant-in-Aid for Scientific Research (Project 17105005, 21750145, and others) from the Ministry of Education, Culture, Sports, Science and Technology (MEXT) of Japanese Government.

Supporting information for this article is available on the WWW under http://dx.doi.org/10.1002/anie.200904876.

an electron-rich *p*-aminophenyl group ($\phi_{FL} = 0.008$). As demonstrated in Figure 1C, however, the fluorescence intensity of the APF phosphate buffer solution was greatly enhanced by applying a positive potential ($0 \leftrightarrow +0.5\,V_{QRE}$, where a silver wire was used as a quasi-reference electrode (QRE)). The onset of the increase in the fluorescence intensity at around $+0.35\,V_{QRE}$ can be easily correlated to the oxidation potential (E_{ox}) of aniline ($+0.36\,V_{QRE}$ ($+0.63\,V_{NHE}$; NHE = normal hydrogen electrode)),[9] which is much lower than that of fluorescein ($+1.1\,V_{NHE}$, Figure S4 in the Supporting Information),[10] thereby supporting the reaction scheme depicted in Figure 1A.

On the basis of these experimental results, we evaluated the photocatalytic activity of individual ETS-10 crystals by imaging the fluorescence generated by oxidized APF molecules during UV irradiation. Figure 2A shows typical transmission and fluorescence images of a single ETS-10 crystal in 500 nM APF phosphate buffer (pH 7.4). As predicted by ensemble experiments, the fluorescence intensity underwent a substantial increase immediately after UV irradiation, with a subsequent slight decrease (inset of Figure 2B).

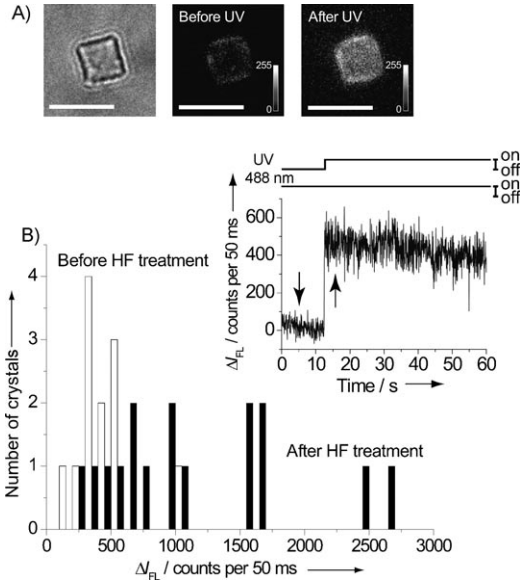

Figure 2. A) Transmission image (left) and fluorescence images of the ETS-10 crystal before (middle) and after UV irradiation (right). The arrows in the inset of (B) denote the times when fluorescence images were acquired. Scale bars are 5 μm. B) Histograms of the increase in fluorescence intensity. The white and black bars indicate histograms obtained for untreated and HF-treated ETS-10 crystals, respectively. Inset shows the time trace of differential fluorescence intensity (ΔI_{FL}), which was obtained by subtracting the background signal from the original intensity averaged over the entire ETS-10 crystal. The intensity before UV irradiation was set to zero.

We investigated the dependence of APF concentration on the fluorescence intensity for a single ETS-10 crystal (Figure S5 in the Supporting Information). Our results showed a clear linear relationship between APF concentration and fluorescence intensity; furthermore, it was estimated that the contribution of scattered light from UV irradiation was approximately 100 counts. From an overall perspective, it appears that the edge of the crystal was relatively more sensitive to UV light than the center, where the imaging focal plane was located. Furthermore, when the crystal was illuminated by evanescent light (penetration depth ca. 200 nm), the entire irradiated area on the bottom surface of the crystal exhibited similar activity as with UV light. Considering the fact that the fluorescein molecule is much larger than the ETS-10 pores, we can conclude that APF molecules are preferentially adsorbed on the exterior surface of ETS-10.[11,12]

To ascertain the origin of reactive species, we performed several control experiments. In the presence of DMSO (5 mM) as an ·OH quencher,[7b] the increase in fluorescence intensity upon UV irradiation was slightly suppressed, thereby indicating that fluorescein molecules generated from the bimolecular reaction between APF and ·OH are not readily detected owing to the rapid diffusion of free fluorescein molecules into the bulk solution.[7b] In contrast, in the presence of aniline (5 mM) as a co-adsorbate, the increase in fluorescence intensity upon UV irradiation was completely suppressed (Figure S6A in the Supporting Information). We also found that there was no significant difference in fluorescence intensity before and after the addition of benzoic acid (5 mM), thus implying that the *p*-aminophenyl group of APF plays an important role in the adsorption on the surface of ETS-10 (Figure S6B in the Supporting Information).[13]

To compare the photocatalytic activity of ETS-10 before and after HF treatment, we examined the histogram of the fluorescence intensity change for individual ETS-10 crystals. As illustrated in Figure 2B, the results for untreated ETS-10 showed a relatively narrow distribution at around 300–500 counts, while HF-treated ETS-10 had a significantly broader distribution (250–2750 counts). We confirmed this increase in fluorescence intensity for a selected ETS-10 crystal in APF buffer solution after HF treatment (Figure S7 in the Supporting Information). Single-crystal Raman spectroscopy measurements also support the hypothesis that the partial dissociation of titania wires in ETS-10 by HF treatment produces the surface active sites (Figure S8 in the Supporting Information).[3]

Experiments on a single crystal provide useful information for elucidating the inherent heterogeneity of reaction processes occurring at the solid–liquid interface. Figure 3 shows an example of the influence of crystal defects on the photocatalytic oxidation of APF molecules. Figure 3A shows transmission (left) and fluorescence (right) images acquired for one single HF-treated ETS-10 crystal. The spatial configuration of the crystal is also illustrated in Figure 3B. To confirm the existence of defects, we carefully analyzed the transmission images acquired at different focal planes.

Figure 3C shows time traces of the fluorescence intensity acquired at a crack-like defect (position 1) and at a point near the edge (position 2). The increase in fluorescence intensity observed at the defect upon UV irradiation is considerably higher than the increase observed at position 2 and other areas. This finding obviously reflects the fact that crystal defects in ETS-10, where titanols and supermicropores are probably present,[5] yield highly active sites for adsorption and oxidation of organic compounds.

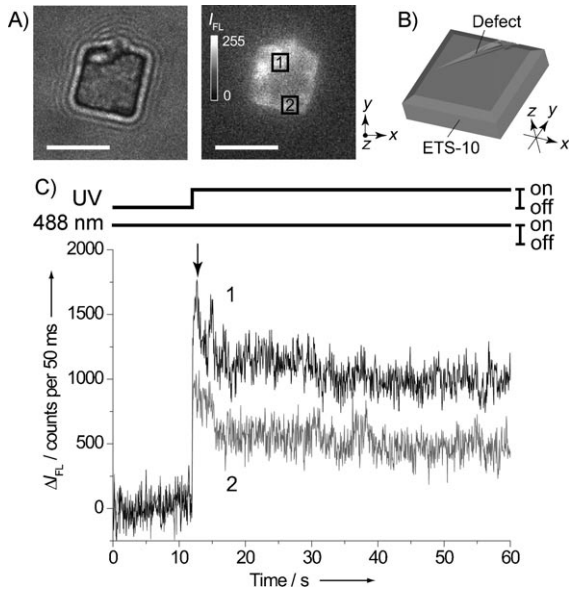

Figure 3. A) Transmission image (left) and fluorescence image under UV irradiation (right), where the imaging focal plane was located at the center of the crystal. The arrow in (C) denotes the time when the fluorescence image was acquired. Scale bars correspond to 5 μm. B) Spatial configuration of the crystal (see the axes). C) Time traces of the fluorescence intensity acquired at the defect (position 1, black line) and near the edge of the ETS-10 crystal (position 2, gray line). Additional data are provided in the Supporting Information (Figure S9).

We further examined the influence of accumulation of intermediates or products on the turnover number for photocatalysis on a single crystal. Figure 4 shows time traces

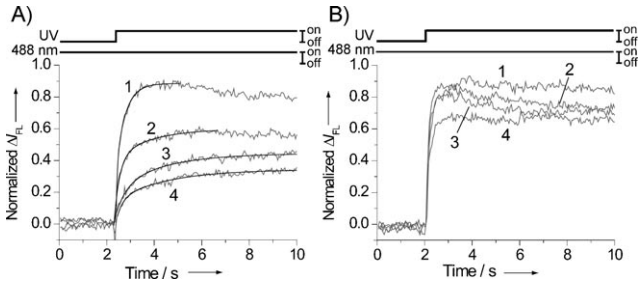

Figure 4. Time traces of fluorescence intensity repeatedly acquired for A) an untreated and B) an HF-treated ETS-10 crystal (gray lines). Numbers refer to the repetition number. Black lines indicate biexponential curves fitted to the time traces.

of the fluorescence intensity acquired repeatedly for the same ETS-10 crystal. For the untreated ETS-10 crystal, the increase in fluorescence intensity was clearly suppressed by repeating a given sequence, that is, flow of substrate solution (40 μL × 3), data acquisition (488 nm laser irradiation for 10 s and UV irradiation for 8 s), and waiting for 1 min (Figure 4A). It is noteworthy that the rise times of fluorescence intensity increased because of frequent repetition.

The time traces were tentatively fitted using a nonlinear least-squares method with a biexponential function given by $I_{FL}(t) = a_1 \exp(-t/\tau_1) + a_2 \exp(-t/\tau_2)$, where I_{FL} is the fluorescence intensity, a is the preexponential factor, and τ is the rise time. As summarized in Table 1, weight-average rise times $\langle\tau\rangle$[14] for untreated ETS-10 increased considerably with an increase in the number of repetitions. On the other hand, as shown in Figure 4B, similar tendencies were not observed for most HF-treated ETS-10 crystals. The $\langle\tau\rangle$ values for HF-treated ETS-10 exhibited no significant change under the same reaction conditions ($\langle\tau\rangle = 100$–200 ms).

Table 1: Fitting parameters for time traces of the fluorescence intensity observed for a single untreated ETS-10 crystal.

Repetition	τ_1 [s] (a_1 [%])	τ_2 [s] (a_2 [%])	$\langle\tau\rangle$ [s][a] ($\langle\tau\rangle^{-1}$ [s^{-1}])
1	0.392 (45)	0.0459 (55)	0.35 (2.9)
2	0.225 (64)	1.54 (36)	1.3 (0.77)
3	0.434 (45)	2.05 (55)	1.8 (0.56)
4	0.244 (45)	2.13 (55)	2.0 (0.50)

[a] Error within ±10%. The response time of the instrument is less than 100 ms.

The photocatalytic reaction mechanism proceeds according to the reactions in Equations (1)–(4):

$$\text{ETS-10} + h\nu \rightarrow e^- + h^+ \quad (1)$$

$$e^- + Ti^{4+} \rightarrow Ti^{3+} \quad (2)$$

$$h^+ + APF_{ads} \rightarrow \text{oxidized } APF_{ads} \text{ (fluorescent form)} \quad (3)$$

$$\text{oxidized } APF_{ads} + h^+ \text{ or ROS} \rightarrow \text{products} \quad (4)$$

Upon irradiation with UV light, the generated electrons (e^-) and holes (h^+) are transferred to electron trapping sites such as Ti^{4+} and APF molecules adsorbed on the surface of the crystal [Eqs. (1–3)]. Both free and surface-trapped h^+ might be included in the oxidation process.[15] Upon oxidation of the *p*-aminophenyl group, APF molecules attain the fluorescent form in a manner similar to the fluorescein molecule. The generated emissive APF-based molecules are further oxidized by h^+ or reactive oxygen species (ROS) to give adsorbed products [Eq. (4)]. This situation should inhibit the adsorption of free APF molecules on the surface, thereby resulting in a decrease in photocatalytic activity. For highly active ETS-10, that is, HF-treated samples, fresh APF molecules are continually supplied to the active sites from the surroundings, because most products are decomposed and desorbed from the surface into the bulk solution.

In conclusion, we have demonstrated in situ fluorescence imaging of photocatalytic active sites heterogeneously distributed on individual ETS-10 crystals using redox-responsive APF molecules. Our strategy can be employed in single-molecule turnover experiments to investigate heterogeneous photocatalysis.[16] Such studies are currently in progress.

Experimental Section

ETS-10 was hydrothermally synthesized according to the procedure reported by Yoon et al.[2] A suspension of anatase TiO_2 nanoparticles was added to a mixture of sodium silicate (8.5 g), sodium hydrate (2.6 g), and Milli-Q water (75 mL) with vigorous stirring. A mixture

of potassium fluoride (1.7 g) and Milli-Q water (15 mL) was added to this mixture, and the resulting suspension was maintained at room temperature for 18 h. A portion of the suspension was heated in a Teflon-lined autoclave at 200 °C for 72 h. The resulting material was separated by centrifugation, repeatedly washed with Milli-Q water until pH 7, and then dried overnight at 90 °C.

Synthesized ETS-10 powder was rapidly mixed with 8 wt % HF, and the mixture was vigorously stirred for 3 s and added into excess Milli-Q water.[3a] (It should be noted that HF is extremely corrosive and behaves as a contact poison; hence, it should be handled with extreme care.) The resulting material was separated by centrifugation, repeatedly washed with Milli-Q water until pH 7, and then dried overnight at 90 °C. Experimental details and spectroscopic data (SEM, powder XRD, and UV/Vis diffuse reflectance spectra) of the ETS-10 materials are provided in the Supporting Information.

For single-molecule, single-crystal fluorescence measurements, an aqueous suspension of ETS-10 crystals was cast on a clean cover glass by spin coating. The coated cover glass was annealed and washed with Milli-Q water. The cover glass was placed on a flow cell built in-house.

The experimental setup for single-particle experiments is based on an Olympus IX71 inverted fluorescence microscope.[7b] Continuous-wave laser light (488 nm) passing through an objective lens (Olympus, UPlanSApo, 1.40 NA, 100×) after reflection at dichroic mirrors was used to excite fluorescent probes. For UV excitation of the sample, light emitted from a 100 W mercury lamp that passed through a 340 nm bandpass filter and a 6% ND filter was made incident on an object lens. For imaging, fluorescence was collected using an objective, passed through emission filters to remove undesirable scattered light, and imaged by an EM-CCD camera (Roper Scientific, Cascade II:512) at a frame rate of 20 frames s^{-1}.

For single-crystal Raman spectroscopy, 532 nm CW laser light passing through an objective lens after reflection at a dichroic mirror was used to excite crystals. The scattered light as well as a background emission was collected using the same objective, passed through an emission filter to remove scattered excitation light and a slit, and entered the imaging spectrograph (Acton Research, SP-2356) that was equipped with an EM-CCD camera (Princeton Instruments, PhotonMAX:512B).

In situ spectroelectrochemical measurements were carried out at room temperature using an electrochemical analyzer (ALS, model 660 A) with a standard three-electrode configuration (Figure S4 in the Supporting Information).[8b] All the experimental data were obtained at room temperature.

Received: September 1, 2009
Published online: November 30, 2009

Keywords: fluorescent probes · heterogeneous catalysis · photochemistry · single-particle studies · zeolite analogues

[1] M. W. Anderson, O. Terasaki, T. Ohsuna, A. Philippou, S. P. MacKay, A. Ferreira, J. Rocha, S. Lidin, *Nature* **1994**, *367*, 347–351.

[2] N. C. Jeong, M. H. Lee, K. B. Yoon, *Angew. Chem.* **2007**, *119*, 5972–5976; *Angew. Chem. Int. Ed.* **2007**, *46*, 5868–5872.

[3] a) F. X. Llabrés i Xamena, P. Calza, C. Lamberti, C. Prestipino, A. Damin, S. Bordiga, E. Pelizzetti, A. Zecchina, *J. Am. Chem. Soc.* **2003**, *125*, 2264–2271; b) S. Usseglio, P. Calza, A. Damin, C. Minero, S. Bordiga, C. Lamberti, E. Pelizzetti, A. Zecchina, *Chem. Mater.* **2006**, *18*, 3412–3424.

[4] P. D. Southon, R. F. Howe, *Chem. Mater.* **2002**, *14*, 4209–4218.

[5] C. C. Pavel, S.-H. Park, A. Dreier, B. Tesche, W. Schmidt, *Chem. Mater.* **2006**, *18*, 3813–3820.

[6] L. Lv, J. K. Zhou, F. Su, X. S. Zhao, *J. Phys. Chem. C* **2007**, *111*, 773–778.

[7] a) K. Setsukinai, Y. Urano, K. Kakinuma, H. J. Majima, T. Nagano, *J. Biol. Chem.* **2003**, *278*, 3170–3175; b) K. Naito, T. Tachikawa, M. Fujitsuka, T. Majima, *J. Am. Chem. Soc.* **2009**, *131*, 934–936; c) V. Martínez Martínez, G. De Cremer, M. B. J. Roeffaers, M. Sliwa, M. Baruah, D. E. De Vos, J. Hofkens, B. F. Sels, *J. Am. Chem. Soc.* **2008**, *130*, 13192–13193.

[8] a) R. E. Palacios, F.-R. F. Fan, A. J. Bard, P. F. Barbara, *J. Am. Chem. Soc.* **2006**, *128*, 9028–9029; b) T. Tachikawa, T. Majima, *J. Am. Chem. Soc.* **2009**, *131*, 8485–8495.

[9] P. Winget, E. J. Weber, C. J. Cramer, D. G. Truhlar, *Phys. Chem. Chem. Phys.* **2000**, *2*, 1231–1239.

[10] J. Suomi, T. Ylinen, M. Håkansson, M. Helin, Q. Jiang, T. Ala-Kleme, S. Kulmala, *J. Electroanal. Chem.* **2006**, *586*, 49–55.

[11] a) As a separate experiment, we studied the adsorption behavior of fluorescein molecules on the surface of ETS-10 powders in solutions, and we estimated the number of adsorbed fluorescein molecules to be less than 5% and approximately 10% of the total molecules (500 nM) in the untreated and HF-treated ETS-10 powders, respectively. Experimental procedures were described elsewhere; b) T. Tachikawa, Y. Asanoi, K. Kawai, S. Tojo, A. Sugimoto, M. Fujitsuka, T. Majima, *Chem. Eur. J.* **2008**, *14*, 1492–1498.

[12] a) In general, when fluorescein molecules are adsorbed on the TiO_2 surface, the fluorescence signals from fluorescein cannot be observed because of the excited-state quenching that accompanies the electron injection into the conduction band of TiO_2. However, taking into account the fact that the band gap energy of ETS-10 is approximately 0.6 eV higher than that of anatase TiO_2 in water at pH 7.4, the driving force for the electron injection (ca. 0.8 eV) might be reduced to near zero; b) D. Duonghong, J. Ramsden, M. Grätzel, *J. Am. Chem. Soc.* **1982**, *104*, 2977–2985.

[13] L. Zang, R. Liu, M. W. Holman, K. T. Nguyen, D. M. Adams, *J. Am. Chem. Soc.* **2002**, *124*, 10640–10641.

[14] D. R. James, Y. S. Liu, P. De Mayo, W. R. Ware, *Chem. Phys. Lett.* **1985**, *120*, 460–465.

[15] T. Tachikawa, M. Fujitsuka, T. Majima, *J. Phys. Chem. C* **2007**, *111*, 5259–5275.

[16] a) M. B. J. Roeffaers, B. F. Sels, H. Uji-i, F. C. De Schryver, P. A. Jacobs, D. E. De Vos, J. Hofkens, *Nature* **2006**, *439*, 572–575; b) W. Xu, J. S. Kong, Y.-T. E. Yeh, P. Chen, *Nat. Mater.* **2008**, *7*, 992–996.

